Molecular Crystals and Liquid Crystals

Publication details, including instructions for authors and subscription information:
http://www.tandfonline.com/loi/gmcl16

Heat Capacity of N-(o-Hydroxy-p-Methoxybenzylidene)-p-Butylaniline: A Glassy Nematic Liquid Crystal

Michio Sorai [a] & SyÛzô Seki [a]

[a] Department of Chemistry Faculty of Science, Osaka University, Toyonaka, Osaka, 560, Japan

Version of record first published: 21 Mar 2007.

To cite this article: Michio Sorai & SyÛzô Seki (1973): Heat Capacity of N-(o-Hydroxy-p-Methoxybenzylidene)-p-Butylaniline: A Glassy Nematic Liquid Crystal, Molecular Crystals and Liquid Crystals, 23:3-4, 299-327

To link to this article: http://dx.doi.org/10.1080/15421407308083379

Molecular Crystals and Liquid Crystals. 1973. Vol. 23, pp. 299–327

Heat Capacity of N-(*o*-Hydroxy-*p*-Methoxybenzylidene)-*p*-Butylaniline: A Glassy Nematic Liquid Crystal†

MICHIO SORAI and SYÛZÔ SEKI

Department of Chemistry
Faculty of Science
Osaka University
Toyonaka, Osaka 560, Japan

Received November 7, 1972; *in revised form January* 22, 1973

Abstract—The heat capacity of N-(2-hydroxy-4-methoxybenzylidene)-4′-butylaniline(2,4-OHMBBA) with a purity of 99.393 mole % was measured between 13 and 375 K. The melting point T_m was 314.30 K, and the enthalpy and the entropy of fusion were 22.405 kJ mol^{-1} and 71.425 J K^{-1} mol^{-1}, respectively. The temperature of transition from nematic to isotropic liquid was 333.65 ± 0.1 K, and the enthalpy and the entropy changes due to this mesophase transition were 887.4 ± 4.9 J mol^{-1} and 2.690 ± 0.015 J K^{-1} mol^{-1}, respectively. A second-order character has been postulated for the mesophase transition.

By cooling the nematic liquid crystal at a rate of − 12.2 K min^{-1} a frozen-in state of the stable nematic phase, i.e. a glassy state, was realized. The glass transition temperature T_g was 204 K and the heat capacity jump at T_g was $\Delta C_p = 107$ J K^{-1} mol^{-1}. The activation enthalpy for the glass transition was estimated to be $\Delta H^* = 75$ kJ mol^{-1}. The residual entropy of the glassy state at 0 K was determined to be 12.69 ± 0.16 J K^{-1} mol^{-1}. The enthalpy of the glassy state at 0 K was 11.38 ± 0.04 kJ mol^{-1} higher than that of crystal. The term *glassy liquid crystal* is proposed here to indicate a glassy state of this kind.

To elucidate the relationship between molecular structure and liquid crystallinity 4 different 2,4-OHMBBA isomers were synthesized. None of them showed liquid crystallinity. From differential thermal analyses it was found that three of them exhibit a glassy state of isotropic liquid: 2,3-OHMBBA ($T_g = 230$ K; $T_m = 320$ K; $\Delta H^* = 85$ kJ mol^{-1}), 2,5-OHMBBA (218 K; 321.7 K; 90 kJ mol^{-1}), and 4,3-OHMBBA (265 K; 357.7 K; 73 kJ mol^{-1}). 3,4-OHMBBA gave no glassy state but a solid–solid transition at 333 K was noted. The material melted at 349 K. 3,4-OHMBBA obtained from the melt exhibited a transition between metastable crystalline phases at 216 K.

---

† Presented by title only at the Fourth International Liquid Crystal Conference, Kent State University, August 21–25, 1972.

1. Introduction

From the viewpoint of the fundamental studies a requisite has been made to find chemically and physically stable liquid crystals having a molecular structure as simple as possible. Most liquid crystals exhibit their mesophase transitions at elevated temperatures. This leads to the thermal decomposition of the materials and gives rise to difficulties in purification.

Since Kelker and Scheurle(1) reported low-temperature nematic liquid crystals of Schiff's bases, similar kinds of materials with relatively simple structures have been found.(2–5) Among them, N-(*o*-hydroxy-*p*-methoxybenzylidene)-*p*-butylaniline (OHMBBA)(2) exhibits a nematic mesophase between 44 and 64.5 °C. This compound has intramolecular hydrogen bonding which stabilizes the anil linkage. Therefore, OHMBBA fulfills the requisites mentioned above.

As one of a series of investigations(6–8) on liquid crystals we have measured precisely the heat capacities of this material between 13 and 375 K by use of an adiabatic calorimeter. The first purpose of the present paper is to study the nature of mesophase transitions from the thermodynamic point of view. Among the vast number of investigations concerning liquid crystals, the number of significant thermodynamic studies is extremely small. As far as the present authors notice, the majority of the thermodynamic studies based on adiabatic calorimetry are found in a series of papers by Arnold *et al.*(9) Calorimetric measurements using the methods of differential thermal analysis (DTA) and differential scanning calorimetry (DSC) have been reported by Barrall, Porter and Johnson(10) and by Ennulat(11) (to list a few).

The second purpose of this paper is to gain some information about the relationship between molecular structure and liquid crystallinity. We have prepared 4 OHMBBA isomers in which the positions of two substituent groups, i.e. hydroxy and methoxy, were altered in turn within the same benzene ring. Thermal properties of these isomers were examined by the methods of DTA and DSC. Although none of them showed liquid crystallinity, a glassy state of the isotropic liquid was realized for three of them.

The third purpose of the present paper is to investigate the glassy state obtained from the supercooled nematic state of OHMBBA. The glassy state of a liquid crystal was first established for cholesteryl hydrogen phthalate (CHP).(7) We proposed a new term *glassy liquid crystal* for the frozen-in state of the supercooled liquid crystalline phase which exhibits a glass transition point. In the case of CHP it was observed only for a metastable mesophase realized through a monotropic transition. In the present case the glassy state was formed from the stable nematic phase. In this paper we present the results of heat capacity measurements on the glassy liquid crystalline state of OHMBBA.

It has been widely recognized through the efforts of many workers that a glass transition may be of quite wide occurrence in condensed matter, and that the concept of glass transition may be understood in terms of a relaxational effect dependent on the particular degrees of freedom in a condensed state. In fact, such transitions may be encountered even in crystalline materials having various molecular,(12) metallic(13) plastic phases and crystals(14,15) with hydrogen-bond networks. Molecular crystals with plastic phases consist of spherical molecules and may be looked upon as isotropic crystals with disordered molecular orientation. Liquid crystals, which consist of elongated and rectilinear molecules, are regarded as anisotropic liquids having a tendency towards ordered orientation. In this respect, it is of interest to compare glassy liquid crystals with glassy crystals.(12)

2. Experimental

MATERIALS

The substances studied here are aromatic Schiff's bases of the type

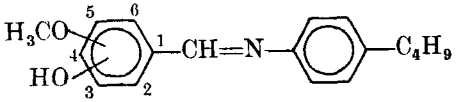

and are denoted generally by N-(x-hydroxy-y-methoxybenzylidene)-p-butylaniline, where x and y represent the positions of the substituent groups. Hereafter, we shall designate these compounds as in an abbreviated form, *x,y*-OHMBBA. Where there is no risk of misinterpretation, the prefixes attached to the nematogenic compound, 2,4-OHMBBA, will be omitted and the simple notation OHMBBA will be used to denote that liquid crystal.

The nematogenic substance, 2,4-OHMBBA,(16) of a special grade was obtained from Tokyo Ohka Kogyo Co., Ltd., purified by recrystallization from pure ethanol and dried in a high vacuum for 24 hours. All other compounds, i.e. 2,3-, 2,5-, 3,4-, and 4,3-OHMBBA, were prepared by the usual condensation reaction in ethanol of *p*-butylaniline (Wako Pure Chemical Industries, Ltd.; Guaranteed Reagent) with the corresponding aldehyde obtained from Wako Pure Chemical Industries, Ltd., Tokyo Kasei Kogyo Co., Ltd., and E. Merck AG. The products were recrystallized two or three times from pure ethanol and dried in the same way. Elementary analyses for these materials were as follows: Calcd. for $C_{18}H_{21}O_2N$ (C, 76.30%; H, 7.47%; N, 4.94%). Found: 2,3-OHMBBA (76.15; 7.47; 4.93); 2,4-OHMBBA (76.34; 7.36; 4.96); 2,5-OHMBBA (76.34; 7.34; 5.01); 3,4-OHMBBA (76.41; 7.46; 5.04); 4,3-OHMBBA (76.38; 7.51; 4.97).

THERMAL ANALYSES

For the preliminary study of the thermal properties of these five materials, differential thermal analyses were carried out between −170 and 100 °C. The amount of specimen used for DTA was about 0.5 g. A detailed description of this apparatus has been given previously.(17)

In order to examine the kinetics around the glass transition, thermal analyses with different heating-rates were made using a differential scanning calorimeter (Perkin–Elmer, DSC-1B) between −100 and 100 °C. The amount of specimen used was about 100 mg.

HEAT CAPACITY MEASUREMENT

The heat capacity of OHMBBA was measured with an adiabatic low-temperature calorimeter(18) between 13 and 375 K. Although the essential parts of this calorimeter system were the same as described previously, slight modifications have been made in the calorimeter cell and the temperature scale. Thermal contact between the platinum resistance thermometer, heater, and sample container was established by use of Apiezon N grease (Associated Electrical Industries, Ltd.; Shell Co.) instead of Wood's alloy. This made possible heat capacity measurements up to 375 K. To reduce the heat capacity anomaly associated with the Apiezon N grease around 300 K (also observed for Apiezon T grease(19)) an equal but minimum quantity of this grease was used in measurements of both the full and the empty calorimeter.

The platinum resistance thermometer (H. Tinsley Co., Ltd.) used in this experiment was calibrated(6) based on the IPTS-68 temperature scale.(20) The deviations of the calibration points from the IPTS-68 scale were within ±0.0015 K.

The all-gold calorimeter cell of approximately 35 cm^3 internal volume contained 15.3364 g (= 0.0541208 mol) of OHMBBA. The empty space was filled with helium gas at 1 atm pressure and room temperature to aid the heat transfer.

MICROSCOPE OBSERVATION

The identification of mesophase for OHMBBA was made using a polarization microscope (Olympas Model TOS) equipped with a hot-stage. Temperature of specimen was determined with a chromel-alumel thermocouple.

3. Thermal Properties

As was reported by Teucher *et al.*,(2) 2,4-OHMBBA exhibits an enantiotropic nematic phase between 44 and 64.5 °C on heating from the crystal and between 64.5 and 8 °C on cooling from the isotropic liquid when the cooling rate was not greater than -10 K min^{-1}. However, the nematic range could be extended to lower temperatures by rapid cooling of the specimen at a rate greater than -10 K min^{-1}. At absolute zero, where the supercooled nematic phase may be regarded as a thermodynamically non-equilibrium glassy state, some residual entropy will be expected. The thermal properties of this nematic substance as studied by DTA have been described in a previous paper.(8) We made an attempt to observe any variations in nematic textures at the supercooled state by use of a polarization microscope with a heating block. However, crystallization of the thin specimen prevented successful observation. In the normal mesophase region typical nematic textures such as threaded texture, nematic droplet, and centered texture were seen between crossed nichols.

Except for 2,4-OHMBBA all other isomers did not exhibit any mesophase on either heating or cooling. As will be discussed in Sec. 6, this fact is probably closely related to the molecular structure. Thermograms for these materials are given in Fig. 1. In this figure

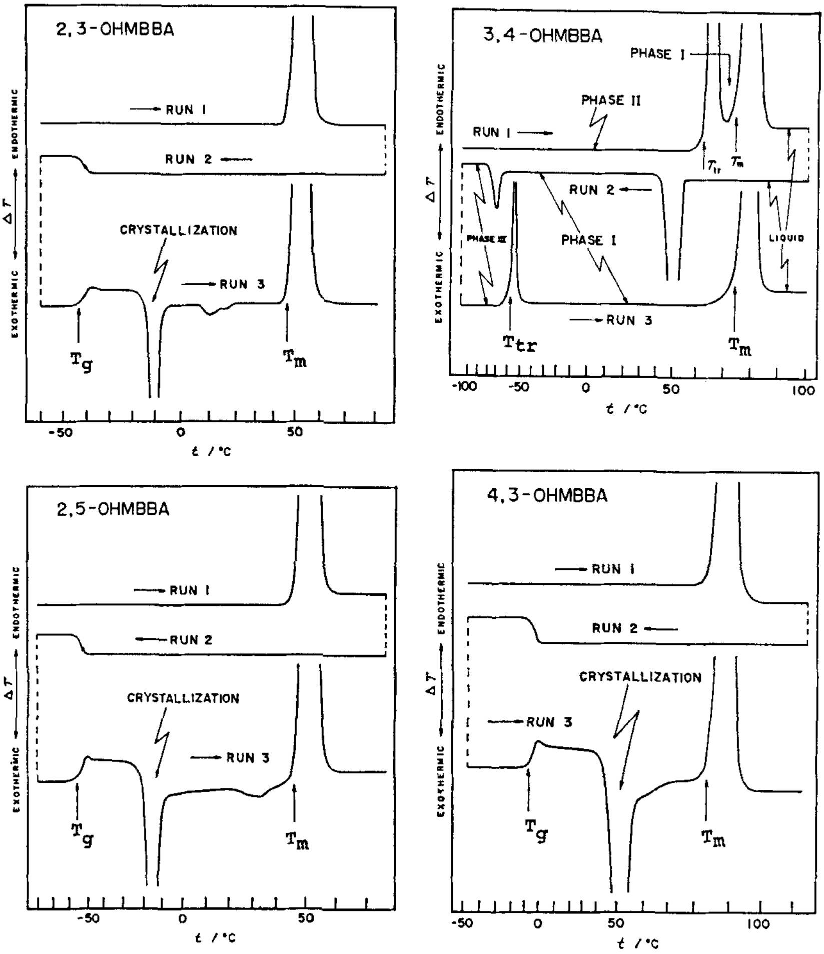

Figure 1. DTA curves for the OHMBBA isomers.

Run 1 shows a heating curve of particular crystalline material at a rate of 2 K min^{-1}, Run 2 gives a cooling curve of the isotropic liquid at a rate of -12 K min^{-1}. Run 3 corresponds to the DTA curves obtained when the rapidly cooled specimens are reheated at a rate of 2 K min^{-1} from the lowest temperature attained.

2,3-, 2,5-, and 4,3-OHMBBA formed a glassy phase from the isotropic liquid. When the temperature was increased these glassy states were transformed into the supercooled liquid states and exhibited typical glass transition phenomena associated with the glass transition temperature T_g. On further heating, the supercooled liquid state was transformed into the stable crystalline phase, which melted at the same temperatures as the original crystals.

In case of 3,4-OHMBBA the cooling rate of -12 K min^{-1} was not great enough to form a glassy state. Of five OHMBBA isomers this is the only material which exhibits polymorphism in solid state. The original crystal, which is designated as Phase II hereafter, underwent a phase transition at 60 °C to give a new Phase I, which melted at 76 °C (see Run 1). The Phase I obtained by cooling from the melt was easily supercooled to -65 °C at which a phase transition into a new Phase III took place (see Run 2). Upon heating the phase transition from III to I occurred at -57 °C, and the crystalline Phase I melted at the same temperature (see Run 3). To promote irreversible transition from the supercooled Phase I to Phase II, the specimen was annealed at 55 °C for 18 h and then left for several days at room temperature. However, no effects of transformation appeared. In order to check whether the sample was decomposed or not, that specimen was recrystallized from pure ethanol. After this the thermal properties were the same as those shown in Fig. 1. It is safe to conclude that Phase II is the stable form below 60 °C, and that the phase transition at -57 °C occurs between two metastable crystalline phases.

To determine activation enthalpy for the glass transformation the effect of heating rate on the glass transition in the glass forming materials of the OHMBBA isomers were examined by use of DSC. The heating rates adopted here were 10, 20, and 40 K min^{-1} and in addition 2.5 and 5 K min^{-1} were used for 2,5-OHMBBA. The results are plotted in Fig. 2, where $\dot{T}_S$ means the heating rate in K min^{-1} and T_g the glass transition temperature defined as the inflection point of DSC curve. According to McMillan⁽²¹⁾ the slopes of the curves in Fig. 2 are related to the activation enthalpy, ΔH^*, necessary for the relaxation process. The numerical values of ΔH^* and the transition temperatures obtained from DTA are summarized in Table 1. Discussions based on these values will be given in Secs. 6 and 7.

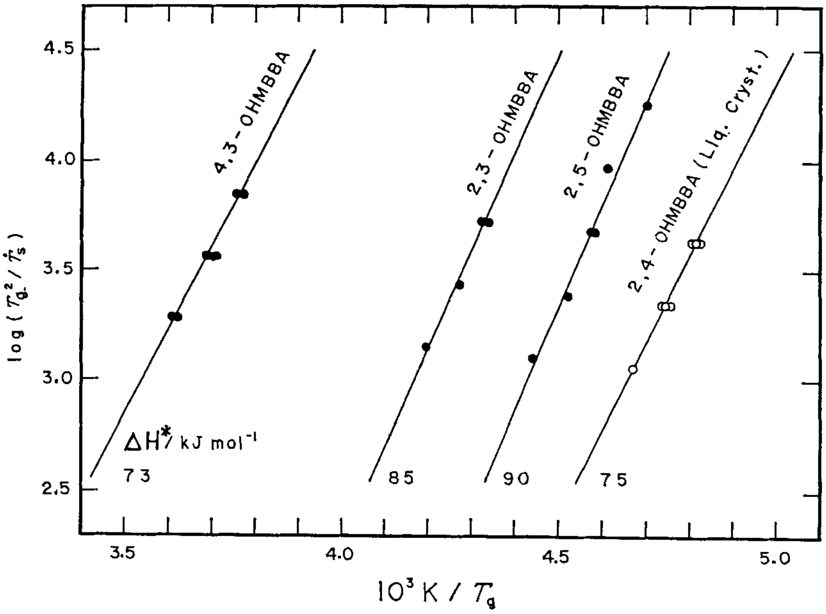

Figure 2. Effect of heating rate on the glass transition temperatures of the OHMBBA isomers.

Table 1 Transition Temperatures[a] and Activation Enthalpy of Glass Transition for the OHMBBA Isomers

Substance	Crystal color	Liquid crystal?	Solid–solid transition?	t_g / °C	t_m / °C	T_g / T_m	ΔH^* / kJ mol⁻¹
2,3-OHMBBA	Orange	No	No	−43	47	0.72	85
2,4-OHMBBA	Yellow	Yes (Nematic)	No	−65	44	0.66	75
2,5-OHMBBA	Orange	No	No	−55	48.5	0.68	90
3,4-OHMBBA	Colorless	No	Yes	—	76	—	—
4,3-OHMBBA	Colorless	No	No	−8	84.5	0.74	73

[a] As seen from the case of 2,4-OHMBBA, the transition temperatures listed here are slightly higher than those obtained from the heat capacity measurement because of the dynamic character of DTA method.

4. Heat Capacity of OHMBBA

The results of the calorimetric measurements have not been converted into the molar heat capacity under the saturation vapor pressure, C_{sat}, due to the lack of data on density, vapor pressure, and heat of vaporization. The present results correspond approximately to the molar heat capacity at constant pressure, C_p, although a minor effect of vaporization of the sample into the narrow empty space of the calorimeter cell may be included in the liquid state. Apart from the absolute values of the heat capacity, the evaluations of the residual entropy and the enthalpy at absolute zero characteristic to the glassy state does not suffer from such a treatment, because we can take the equilibrium nematic or isotropic liquid states as a reference state for these calculations. The experimental data are listed in Tables 2 and 3 and plotted in Fig. 3.

The first series of heat capacity measurements were started at 13 K for the crystalline state and continued up to 375 K. Then, the isotropic liquid was cooled very slowly down to 287 K. The second series of measurements were carried out for the supercooled nematic state thus obtained.

In addition to the heat capacity measurements several independent calorimetric measurements were made to determine the purity of the present specimen, the heat of fusion, and the heat of transition. With the knowledge of the enthalpy change from crystal to nematic state, the concentration of liquid–soluble solid–insoluble impurities in the calorimetric sample was calculated to be 0.607 mole %. The melting point, T_{m}, of the present sample is 314.30 K and that of pure 2,4-OHMBBA, $T_{\mathrm{m}}{}^{\circ}$, is 314.52 K. The temperature of transition, T_{C}, from nematic to isotropic liquid was determined graphically to be 333.65 ± 0.1 K. The enthalpy and the entropy changes associated with the fusion and the mesophase transition are summarized in Table 4.

As seen from Fig. 3, the "pretransitional effects"(22–24) are remarkable in the present mesophase system. The excess heat capacity due to phase transition is seen down to rather low temperatures. In the calculation of the enthalpy and the entropy of mesophase transition, we have assumed as the normal heat capacity a straight line which connects the C_p value at 303.610 K and that at

TABLE 2 Heat Capacities of Crystalline, Nematic, and Isotropic Liquid Phases of N-(*o*-Hydroxy-*p*-Methoxybenzylidene)-*p*-Butylaniline (Molecular Weight 283.3736)

$\frac{T}{\mathrm{K}}$	$\frac{C_p}{\mathrm{J\ K^{-1}\ mol^{-1}}}$	$\frac{T}{\mathrm{K}}$	$\frac{C_p}{\mathrm{J\ K^{-1}\ mol^{-1}}}$
14.433	10.677	80.114	128.457
15.344	12.373	82.978	132.548
16.159	13.915	86.107	137.019
16.924	15.292	89.291	141.482
17.794	16.854	92.395	145.743
18.756	18.615	95.427	149.994
19.696	20.428	98.466	154.091
20.689	22.425	101.626	158.204
21.788	24.583	104.957	162.531
23.024	27.079	108.439	166.938
24.378	29.699	111.945	171.450
25.800	32.625	115.385	175.822
27.586	36.269	118.753	180.227
29.689	40.356	122.565	184.697
31.765	44.813	126.768	190.019
33.858	49.104	130.887	195.047
35.996	53.469	134.932	200.158
38.212	57.614	138.911	204.908
40.548	61.881	143.215	210.276
42.948	66.463	147.833	215.944
45.340	71.216	152.426	221.729
47.731	75.529	157.000	227.464
50.134	79.779	161.507	232.823
52.558	83.955	165.949	238.640
54.730	88.024	170.330	243.782
56.914	91.694	174.654	249.191
59.739	96.180	178.920	254.458
63.009	101.747	183.134	259.990
66.251	107.807	186.507	263.866
69.337	112.519	190.875	270.101
72.407	117.138	195.525	275.931
75.473	121.723	200.810	283.003
78.435	126.081	206.360	290.348

$\frac{T}{K}$	$\frac{C_p}{J\ K^{-1}\ mol^{-1}}$	$\frac{T}{K}$	$\frac{C_p}{J\ K^{-1}\ mol^{-1}}$
211.825	297.605	314.195	50502.3
217.209	305.037	314.250	60200.7
221.783	312.164	314.862	2440.68
224.412	315.093	316.373	520.390
228.320	321.224	318.224	523.646
233.466	328.631	320.067	527.698
238.611	336.319	321.728	530.079
243.755	344.131	321.904	530.454
248.829	352.069	324.634	537.438
253.843	360.194	326.319	543.568
258.795	368.507	328.229	551.954
263.667	376.195	330.188	563.659
268.468	384.869	330.497	566.487
273.200	392.720	331.350	572.780
277.865	400.847	332.073	590.788
280.765	404.898	332.290	593.347
282.463	408.991	332.771	646.159
286.003	415.320	333.225	788.454
291.153	424.091	333.385	880.351
292.328	425.758	333.937	771.476
296.215	435.530	333.982	704.727
297.352	437.945	334.678	546.929
297.788	440.557	335.301	540.473
300.244	447.471	335.430	540.064
302.259	462.369	336.023	537.235
306.948	520.960	336.926	537.218
310.159	702.037	338.170	536.935
311.493	981.728	339.988	536.558
312.180	1408.59	342.961	535.819
312.692	2090.33	347.070	538.513
313.139	3406.88	351.604	540.585
313.515	5771.01	356.444	544.028
313.749	9313.21	361.586	547.065
313.901	14166.7	366.708	552.742
314.025	21660.9	371.799	552.694
314.128	35685.2		

Table 3 Heat Capacities of the Glassy and the Supercooled Liquid Crystalline Phases of N-(*o*-Hydroxy-*p*-Methoxybenzylidene)-*p*-Butylaniline (Molecular Weight 283.3736)

$\frac{T}{\mathrm{K}}$	$\frac{C_p}{\mathrm{J\ K^{-1}\ mol^{-1}}}$	$\frac{T}{\mathrm{K}}$	$\frac{C_p}{\mathrm{J\ K^{-1}\ mol^{-1}}}$
14.082	15.237	87.345	142.616
14.920	17.367	90.476	146.815
15.375	18.670	92.188	149.419
15.708	19.297	94.753	152.562
16.053	20.017	97.863	157.126
16.485	20.569	101.337	161.588
16.715	21.335	105.150	166.682
17.288	22.424	109.288	172.156
17.382	22.455	113.427	177.520
18.075	24.021	117.578	182.837
18.259	24.187	121.756	188.100
18.822	25.403	125.963	193.471
19.394	26.438	130.089	198.720
19.768	27.313	132.855	202.466
20.572	28.863	136.901	208.017
20.895	29.674	140.872	212.873
22.134	32.218	144.766	217.867
22.172	32.247	148.969	223.110
24.188	36.238	153.483	228.891
24.963	38.262	157.925	234.434
26.185	40.321	162.302	240.221
27.030	42.127	166.613	246.001
28.142	44.144	170.863	251.473
29.719	47.540	175.051	258.365
30.212	48.246	178.196	262.984
32.554	52.936	180.275	264.473
32.734	53.461	182.514	268.808
35.102	57.852	184.915	271.222
36.178	60.020	187.305	275.084
37.763	62.884	189.680	278.970
39.768	66.566	192.042	283.738
40.442	67.607	194.396	288.267
43.030	72.518	196.737	293.643
45.563	77.152	199.057	302.877
48.090	81.552	201.326	321.764
50.614	85.879	203.418	387.990
53.126	90.162	205.357	408.350
53.636	91.164	207,266	408.102
55.644	94.563	209.362	409.992
56.499	95.920	212.028	411.135
59.686	101.064	214.823	414.533
62.820	106.178	292.180	487.833
65.895	111.028	295.733	492.328
68.958	115.587	299.439	497.890
71.960	120.139	303.610	502.040
74.948	124.478	308.075	508.127
77.992	129.326	312.517	514.016
81.073	133.598	317.070	520.871
84.202	138.096		

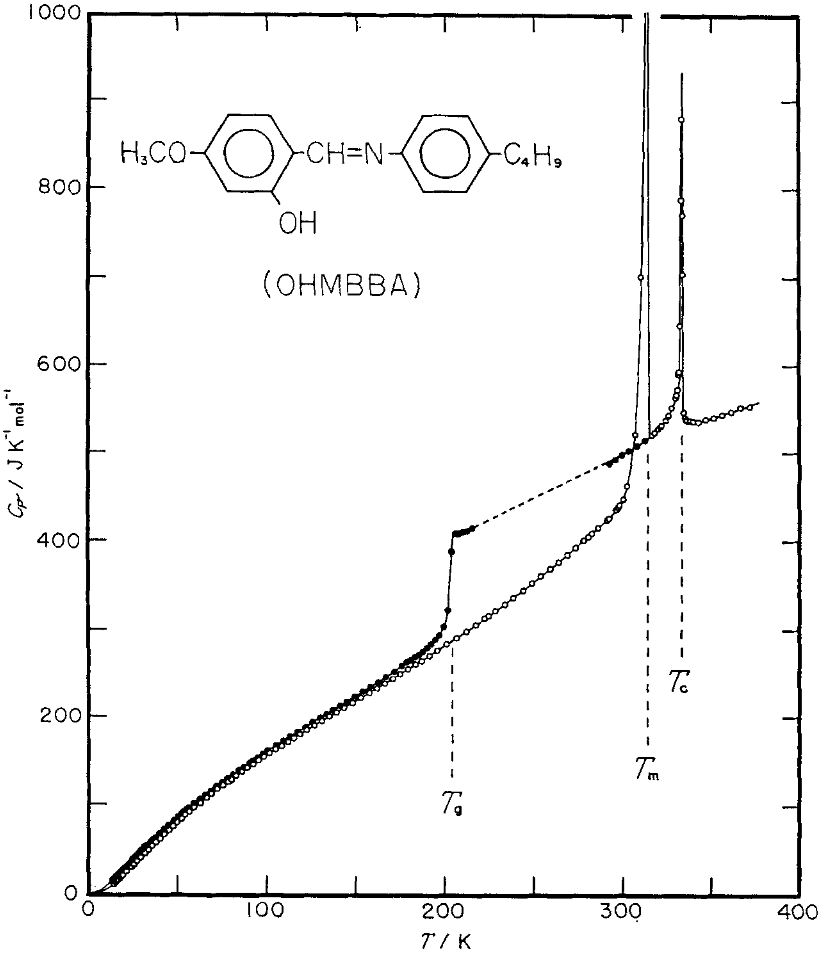

Figure 3. Molar heat capacities of 2,4-OHMBBA. ○ : crystal, nematic, and isotropic liquid. ● : the glassy liquid crystal and the supercooled liquid crystal of the nematic phase.

351.604 K. Detailed discussions concerning the pretransitional effects and the order of phase transition will be given in Sec. 5.

The glassy liquid crystalline state was formed by cooling the sample at an average rate of -12.2 K min^{-1} from the isotropic liquid at 375–120 K. As was pointed out previously,(8) the transition from the isotropic liquid to the nematic phase takes place reproducibly even at a rate as fast as -80 K min^{-1}. This is the

TABLE 4 Enthalpy and Entropy of Transition for 2,4-OHMBBA

Transition	$\frac{T}{\mathrm{K}}$	$\frac{\Delta H}{\mathrm{kJ\ mol^{-1}}}$	$\frac{\Delta S}{\mathrm{J\ K^{-1}\ mol^{-1}}}$
Crystal→Nematic (T_m)	314.30[a]	22.405	71.425
Nematic→Isotropic liquid (T_C)	333.65 ±0.1	0.8874 ±0.0049	2.690 ±0.015

[a] Melting point for the pure material $T_m{}^\circ = 314.52$ K.

reason why we did not start from the nematic state in place of the isotropic liquid in order to establish the glassy liquid crystal. The third series was begun from 13 K for this glassy state. In the glass transition region, a temperature drift arising from heat evolution due to the relaxation of enthalpy was observed. This phenomenon was detected from about 175 K and gradually increased up to about 204 K. Near this temperature the sign of temperature drift dT/dt, where T is the temperature and t the time, changed from plus to minus. The negative drift continued for a temperature interval of one Kelvin or so and the vanishing drift, which is normal in this temperature region for the present calorimeter, was recovered. On calculating the heat capacities, this heat evolution and absorption due to relaxation effects was removed by the correction of temperature drift. The glass transition point, T_g, defined here as a temperature where a sign of temperature drift changes, was determined to be 204 K, and the heat capacity jump at T_g was 107 J K^{-1} mol^{-1}.

When a temperature of a specimen reached about 220 K a large evolution of heat was noted due to the irreversible transition from the supercooled nematic phase to the metastable crystalline phase. After the crystallization was completed, the subsequent evolution of heat due to the irreversible transition from the metastable to the stable crystalline phase occurred.(8) On account of these effects, the heat capacities of supercooled nematic liquid crystal between 215 and 280 K could not be measured.

The heat capacity of the supercooled nematic state between 215 and 280 K was estimated from the following equation

$$C_p = 0.97581T + (206.13 \pm 0.43)\ \mathrm{J\ K^{-1}\ mol^{-1}}. \tag{1}$$

This corresponds to a straight line obtained by connecting the C_p

values at 209.362 and 299.439 K as shown by a broken line in Fig. 3. By use of this interpolation equation the molar enthalpy of the supercooled nematic state referred to that of crystalline state may be determined. The absolute values of enthalpy for both the crystalline and the supercooled nematic states can be obtained if we take the enthalpy value of the crystal at 0 K as zero for the standard point of the enthalpy. In order to check the validity of Eq. (1) we have attempted the following procedures: If the temperature of supercooled nematic state is elevated above T_g, which we designate as T_i (indicating the initial temperature), a spontaneous exothermic transition takes place to a metastable crystalline state which is finally transformed into the stable crystal. If adiabatic conditions are maintained during the irreversible changes and the final temperature, T_f, at which the irreversible transitions will terminate, is measured, the heat content possessed by the supercooled nematic liquid crystal and the calorimeter cell at T_i should be equal to the heat content of the crystal and the cell at T_f. Moreover, if we introduce a reference temperature, T_r, above the melting point, T_m, the enthalpy difference for the former between T_r and T_i should be equal to that for the latter between T_r and T_f;

$$\int_{Ti}^{Tr} C_p(\text{nematic})\,\mathrm{d}T = \int_{Tf}^{Tr} C_p(\text{crystal})\,\mathrm{d}T - n\int_{Ti}^{Tf} C_p(\text{empty cell})\,\mathrm{d}T, \tag{2}$$

where C_p(nematic) and C_p(crystal) are the molar heat capacities starting from the supercooled nematic state at T_i and from the crystal at T_f, respectively, C_p(empty cell) the heat capacity of the empty cell, and n the mole factor equal to 1/0.0541208. In the calculation of these integrals we adopted the values of $T_i = 213.552$ K, $T_f = 234.632$ K, and $T_r = 321.904$ K. In this case the right-hand side of Eq. (2) amounted to 50748.4 J mol^{-1} while the left-hand side was 50670.4 J mol^{-1}. The agreement between them is very satisfactory since the difference is only 78.0 J mol^{-1}. If this amount of enthalpy is distributed with an equal weight over the interpolation region, i.e. 213.552 ~ 299.439 K, the deviation of C_p from Eq. (1) is 0.2% which is approximately equal to the error limits for the present study.

Estimations of the heat capacities below 13 K for the crystal and for the glassy liquid crystal were made using effective frequency spectra.(25) The principle of this method is to seek an effective frequency distribution spectrum with a minimum root-mean-square error among many spectra each of which is determined by the least-square method so as to approximate the experimental heat capacities. The only necessary preset-parameters in this method are the Debye

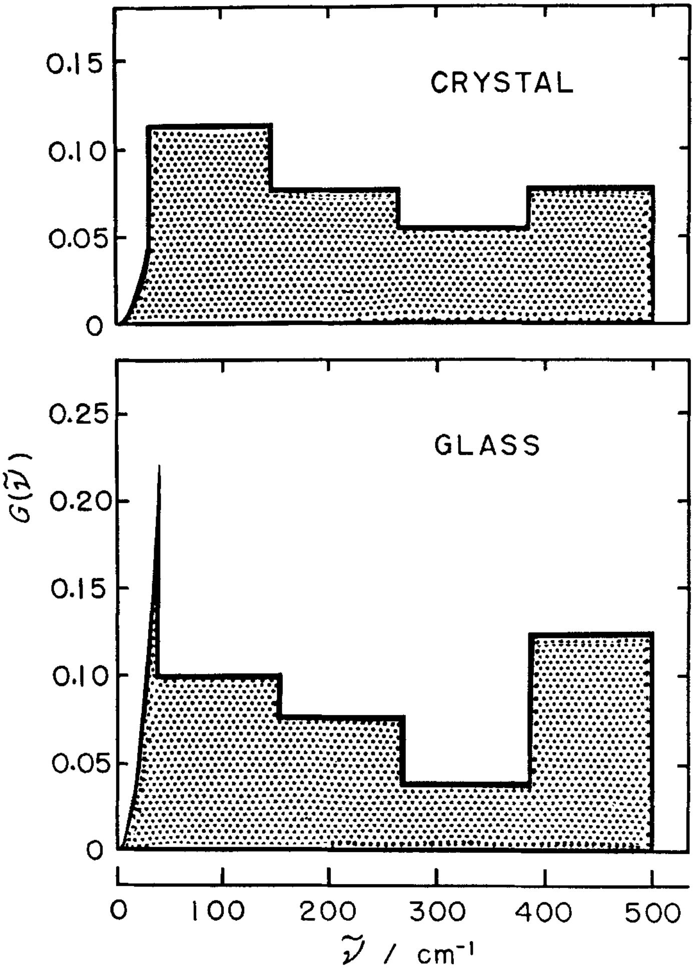

Figure 4. Effective frequency spectra for the crystal and for the glassy liquid crystal, which reproduce the experimental C_p values of OHMBBA below 100 K.

Table 5 Thermodynamic Functions of OHMBBA (in the Unit of J K^{-1} mol^{-1})

$\frac{T}{K}$	$C_p°$	$S°$	$\frac{H° - H_0°}{T}$	$\frac{-(G° - H_0°)}{T}$
		(Crystal)		
5	0.469	0.153	0.115	0.038
10	4.216	1.361	1.033	0.328
15	11.769	4.409	3.280	1.130
20	21.069	9.044	6.543	2.501
25	31.031	14.809	10.438	4.370
30	41.160	21.362	14.714	6.647
35	51.191	28.462	19.211	9.251
40	60.985	35.940	23.824	12.117
45	70.473	43.674	28.483	15.191
50	79.634	51.576	33.142	18.434
60	96.994	67.648	42.355	25.293
70	113.19	83.830	51.330	32.500
80	128.37	99.947	60.022	39.925
90	142.62	115.90	68.416	47.482
100	155.98	131.62	76.512	55.112
110	168.95	147.10	84.350	62.752
120	181.69	162.35	91.933	70.417
130	193.96	177.38	99.305	78.070
140	206.27	192.20	106.51	85.691
150	218.67	206.86	113.58	93.273
160	231.03	221.37	120.54	100.83
170	243.40	235.75	127.40	108.36
180	255.88	250.02	134.19	115.82
190	268.85	264.19	140.93	123.26
200	281.92	278.31	147.65	130.66
210	295.18	292.39	154.37	138.02
220	309.39	306.44	161.08	145.36
230	323.64	320.50	167.84	152.66
240	338.43	334.59	174.63	159.95
250	353.97	348.71	181.49	167.22
260	370.41	362.92	188.44	174.48
270	387.41	377.21	195.49	181.72
280	404.63	391.60	202.65	188.96
290	422.35	406.11	209.91	196.20
300	451.12	420.77	217.32	203.44
310	693.10	437.40	226.69	210.71
314.296		Fusion		
		(Nematic Liquid Crystal)		
318	523.25	519.39	301.92	217.47
320	526.43	522.68	303.31	219.37
322	530.70	525.97	304.71	221.26
324	535.82	529.28	306.13	223.14
326	542.41	532.59	307.55	225.04
328	550.95	535.94	309.02	226.92
330	562.53	539.30	310.49	228.81
333.65		Transition from nematic to isotropic liquid		
		(Isotropic Liquid)		
340	536.56	556.76	318.55	238.20
350	539.85	572.34	324.82	247.52
360	546.13	587.64	330.88	256.75
370	552.67	602.69	336.78	265.91

TABLE 6 Thermodynamic Functions of the Glassy and the Supercooled Liquid Crystalline States of OHMBBA (in the Unit of J K^{-1} mol^{-1})

$\frac{T}{K}$	$C_p°$	$S° - S_0°(\text{vit})$	$\frac{H° - H_0°(\text{vit})}{T}$	$-\frac{(G° - H_0°(\text{vit}))}{T}$
		(Glassy Liquid Crystal)		
5	1.242	0.416	0.312	0.104
10	7.887	3.010	2.216	0.794
15	17.624	8.007	5.695	2.312
20	27.862	14.479	9.957	4.522
25	38.008	21.789	14.555	7.234
30	47.941	29.602	19.296	10.305
35	57.633	37.723	24.084	13.693
40	67.035	46.036	28.868	17.168
45	76.128	54.460	33.617	20.843
50	84.908	62.938	38.310	24.628
60	101.58	79.909	47.481	32.428
70	117.23	96.755	56.338	40.416
80	132.09	113.39	64.886	48.501
90	146.18	129.77	73.155	56.611
100	159.87	145.88	81.159	64.722
110	173.08	161.74	88.912	72.826
120	185.89	177.35	96.472	80.876
130	198.61	192.73	103.82	88.914
140	211.81	207.94	111.08	96.861
150	224.43	222.99	118.22	104.76
160	237.18	237.88	125.26	112.61
170	250.36	252.65	132.23	120.43
180	264.28	267.39	139.20	128.19
190	279.62	282.09	146.18	135.91
200	310.73	296.99	153.41	143.58
204.4		Glass Transition		
		(Supercooled Nematic Liquid)		
210	411.05	315.67	164.35	151.32
220	420.81	335.02	175.79	159.23
230	430.56	353.94	186.65	167.29
240	440.32	372.47	197.02	175.45
250	450.08	390.64	206.95	183.70
260	459.84	408.48	216.49	192.00
270	469.60	426.02	225.68	200.34
280	479.35	443.28	234.57	208.71
290	489.11	460.27	243.17	217.09
300	498.87	477.01	251.53	225.48
310	510.68	493.55	259.69	233.86
315	517.75	501.77	263.73	238.04
320[a]	526.43	509.99	267.76	242.23

[a] Above this temperature the heat capacity of supercooled nematic liquid coincides with the heat capacity started from crystalline state.

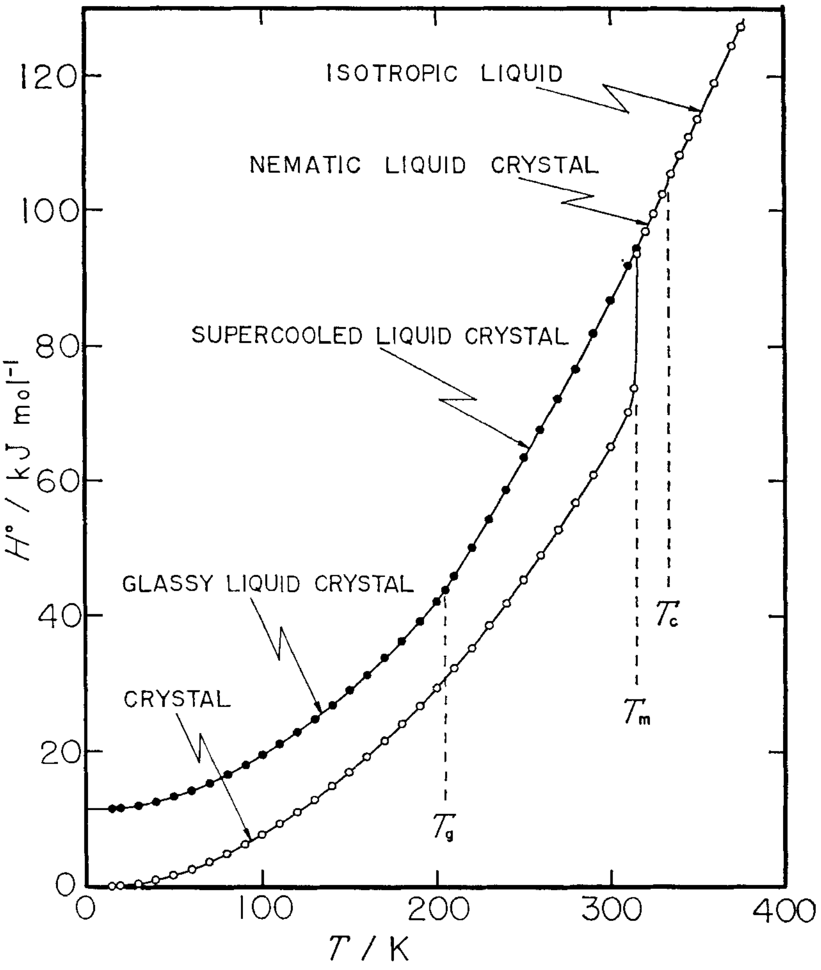

Figure 5. The enthalpy diagram relating various phases of OHMBBA.

cut-off frequency, the Einstein cut-off frequency, and the number of frequency-divisions. We have calculated six spectra for the crystalline state by using 40 C_p values below 100 K and eight spectra for the glassy state using 50 C_p data below 90 K. The best results are given in Fig. 4. This frequency spectrum can reproduce the experimental C_p values of the crystal within the deviation of ± 0.170 J K^{-1}

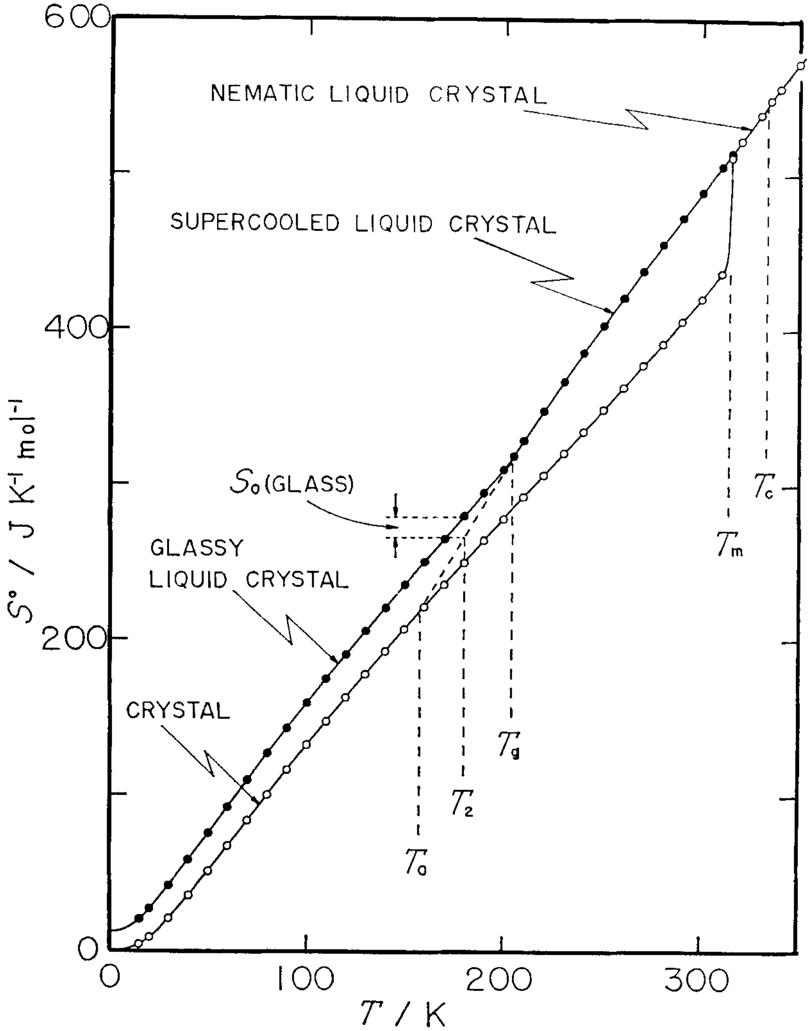

Figure 6. The entropy diagram relating various phases of OHMBBA.

mol^{-1} between 13 and 100 K, and for the glassy state the deviations are within ± 0.147 J K^{-1} mol^{-1} over a region of 13 ~ 90 K.

Thermodynamic functions for the stable phases are listed in Table 5 and those for the glassy and the supercooled nematic states are given in Table 6. Figures 5 and 6 are respectively the enthalpy and the entropy diagrams relating various phases of OHMBBA.

5. Mesophase Transition

Various kinds of experimental results related to mesophase transitions have been interpreted so that mesophase transitions appear to be first order. In a recent review monograph(26) we encounter the following " Liquid crystalline phase transitions are typically first order with latent heats of so many kcal/mol." Observations of latent heat and thermal hysteresis or supercooling are probably the conclusive factors by which one may test for the presence of a first-order nature in the relevant phase transition. However, it is difficult to judge experimentally whether the latent heat was truly observed or not in a mesophase transition. The enthalpy change arising from mesophase transitions is usually very small compared with that of fusion, and the behavior of a mesophase transition may be affected by the impurities involved in the system as may a solid phase be similarly altered. The existing theories dealing with mesophase transitions have also supported the concept of a first order transition, though the theoretical results depend substantially on the approximations and/or the models adopted there.

In the present case of OHMBBA no detectable supercooling of the melt at isotropic–nematic transition occurred at all. The time required for thermal equilibrium after an energy input in the heat capacity measurements was not affected by the mesophase transition. The concentration of impurity in OHMBBA does not seem to be so high as to blur the first-order nature. The same was true for the mesophase transitions in cholesteryl myristate.(6) Thus it may be concluded from the present and also from the previous(6) heat capacity measurements that the mesophase transitions might bear the second- or the much higher-order nature.

Recently McMillan(27) has proposed an interesting model to interpret the mesophase transitions between smectic *A* and nematic and also between nematic and isotropic liquid. One striking feature of his theoretical model is that it predicts possible second-order mesophase transitions under suitable conditions of other parameters such as transition temperatures and/or entropies. Indeed, experimental evidence has been given for a possible second-order mesophase transition between smectic *A* and nematic(28) and between nematic and isotropic liquid.(29) Another prediction derived from the

McMillan theory is a constant entropy of transition (3.56 J K^{-1} mol^{-1}) at the nematic–isotropic–liquid transition. It should be remarked here that the transition entropy of the present material is 2.690 ± 0.015 J K^{-1} mol^{-1} and that our experiment seems to be favorable for his theory.

In relation to the order of mesophase transition there exist " pre- and post-transitional effects " characteristic to mesophase transition. As was mentioned in Sec. 4, the excess heat capacities due to mesophase transition from nematic to isotropic liquid were observed from much lower temperatures below T_C and terminated at a much higher temperature above T_C. The existence of " pre- and post-transition effects " in a phase transition of the second order is natural, but such an expression has never been used to describe the anomalous changes in properties near a critical temperature. On the other hand, to those(22–24) who regard the mesophase transitions as first order, the widespread anomaly near transition temperature may be explained in terms of pre- and post-transition effects, which might be virtually the same as the Frenkel theory(30) of heterophase fluctuations. Whether the anomalous changes near the mesophase transition are regarded as pre- and post-transition effects or not, the anomaly might be caused by low energy fluctuations in the degree and orientation of alignment of the molecules and by the effect of short range orientational interactions.

6. Molecular Structure and Liquid Crystallinity

We shall consider here the problem of why all other isomers except for 2,4-OHMBBA did not exhibit liquid crystallinity. In order to make the following discussions easier, the molecular structures of these isomers are shown schematically in Fig. 7. In this figure the magnitude of dipole moments(31) are shown as the length of arrows and the possible hydrogen bonds are indicated by a segment of thick broken line. Though there is no experimental evidence, the methoxy group seems to undergo a free or a hindered rotation about the axis of O—C(ring) bond in a fluid state. If this is the case, the direction of dipole moment associated with the methoxy group would be parallel to the O—C(ring) bond axis.

On this basis it is easily accepted that 2,4-OHMBBA fulfills the

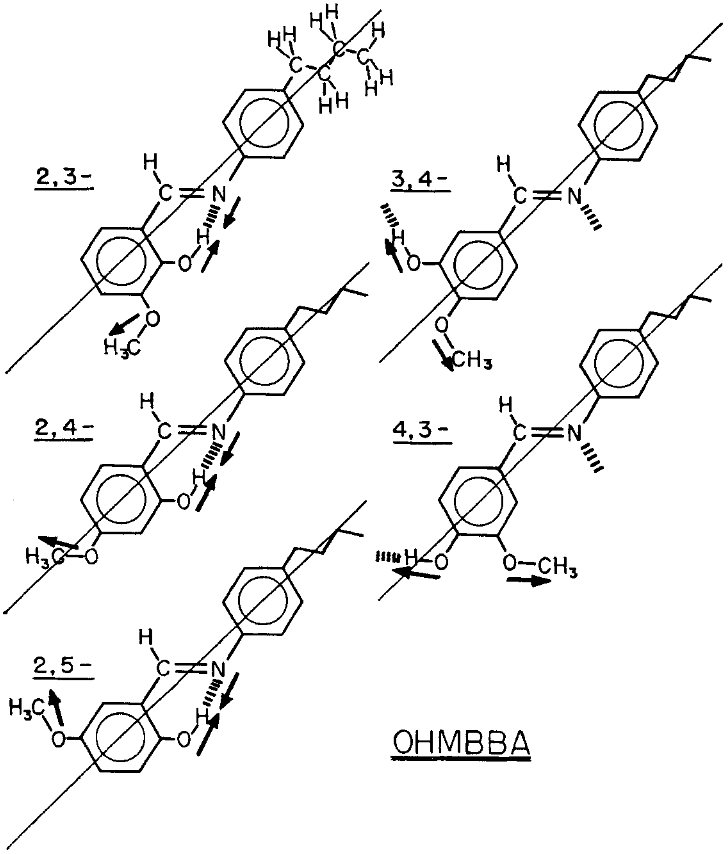

Figure 7. Schematic diagrams of molecular structure for five OHMBBA isomers. The lengths of arrows correspond approximately to the magnitude of dipole moment. A segment of thick broken line indicates a hydrogen bond which might be present.

empirical criterions(26) for liquid crystallinity because the dipole moments arising from O—H...N bonds may be canceled by a formation of an intramolecular hydrogen bond. The resultant strong dipole due to $—OCH_3$ group is located on the molecular axis.

In case of 2,3- and 2,5-OHMBBA the dipole moment due to the methoxy group acts at an angle across the major molecular axis and the shape of molecule is not rectilinear but bent. These facts seem to be the main reasons why these two isomers do not exhibit any liquid crystallinity.

For 3,4- and 4,3-OHMBBA, on the other hand, we at first expected liquid crystallinity since the dipole of the methoxy or the hydroxy group at para-position is strenghthened by that of the hydroxy or the methoxy group located at the adjacent position. But this is not the case. One of the explanations for non-liquid-crystallinity is to say that the intermolecular hydrogen bonds might prevent the molecules from aligning with parallel orientations in a liquid state. The possible existence of such hydrogen bonds in the solid state is obvious from the higher melting temperatures listed in Table 1. If the hydroxy group were replaced by another suitable group, which does not form any hydrogen bond, such a new compound would probably exhibit liquid crystallinity.

7. Glassy Liquid Crystal of OHMBBA

As was mentioned in Sec. 1, the formation of a non-equilibrium glassy state from the nematic phase of OHMBBA is the second example of the so-called glassy liquid crystal yet presented.(7,8) Precise thermodynamic quantities are given for the first time in this paper. In this section we will confine our discussions to the subject " What are the unique and characteristic points for the glassy liquid crystal compared with the ordinary glass or the glassy crystal? "

One of the most important thermodynamic properties of glass is the residual entropy at 0 K, which approximates the configurational entropy of the supercooled state frozen-in at the glass transition temperature. The residual entropy of the present glassy liquid crystal was determined to be $S_0(\text{vit}) = 12.70 \pm 0.16$ J K^{-1} mol^{-1} by using the values listed in Tables 5 and 6. The enthalpy difference at 0 K was $H_0(\text{vitreous state}) - H_0{}^{\circ}(\text{crystalline state}) = 11.38 \pm 0.04$ kJ mol^{-1}.

The residual entropies determined for ordinary glassy liquids are, for example, diethyl phthalate (23 J K^{-1} mol^{-1}),(32) glycerol (19.2),(33) *o*-terphenyl (15),(34) isopentane (14.06),(35) propane-l-ol (11.34),(36) 2-methyl propane-l-ol (9.00),(36) and methanol (7.07).(37) The residual entropies for the known glassy crystals are as follows: *cis*-1,2-dimethylcyclohexane (8.6 J K^{-1} mol^{-1}),(12c,38) 2,3-dimethylbutane

(7.4),(12c) cyclohexanol (4.7),(12a) and cycloheptanol (0.7).(12d) The residual entropies for glassy crystals are much smaller than those for glassy liquids. The border line separating them seems to be 7 or 8 J K^{-1} mol^{-1}. The present result (12.70 J K^{-1} mol^{-1}) obtained for the glassy liquid crystal of OHMBBA is intermediate between them, although it is on the glassy liquid side. This fact may be explained if we consider the situation as follows: For the glassy crystals the configurational degrees of freedoms frozen-in at T_g would consist mainly of the conformational, the internal rotational, the overall molecular orientation, etc.,(12a) while for the ordinary glassy liquid an additional degree of freedom such as the translational modes due to molecules and/or defect-holes would take part in the residual entropy. In the case of glassy liquid crystal the degrees of freedom frozen-in at T_g will be reduced compared with those for the glassy liquid because a higher degree of orientational order has been established in the liquid crystalline state. However, the quenched degrees of freedom will be greater than those for the glassy crystal because there exists no positional order in the liquid crystalline state.

Another parameter, phenomenological in nature, to aid the understanding of the vitreous state of substances in general may be the T_2 temperature defined by Gibbs and DiMarzio.(39) The value of T_2 was determined to be 180 K for OHMBBA (see Fig. 6) and the ratio T_g/T_2 was 1.13. The values of T_g/T_2 for ordinary glassy liquids are within the range of 1.30 ± 0.11,(40) while a different range, 1.15 ~ 1.20, has been reported for the glassy crystals.(12c) It is a remarkable fact that the present material has the smallest value of T_g/T_2 in comparison to the glassy crystals and the glassy liquids given above.

In connection with the value of T_2, one striking feature for the nematic glassy state is a large deviation of the $T_0(=157\ \mathrm{K})$ temperature defined by Angell(41) from T_2 (see Fig. 6). According to him T_0 is defined as a temperature below which the entropy of the supercooled state becomes smaller compared with that of the crystal. The large departure of T_0 from T_2 corresponds to the fact that the heat capacity of the glassy liquid crystal is much higher than that of the crystal. The excess heat capacities $\Delta C_p(=C_p(\text{glass})-C_p(\text{crystal}))$ are plotted in Fig. 8. From 80 K upwards the heat capacity of the glass is about 2.5% ~ 3% higher than that of the

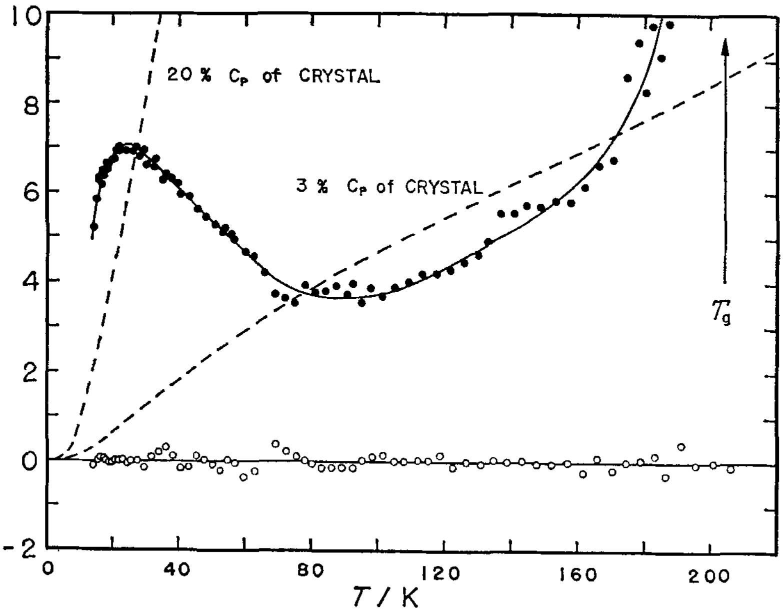

Figure 8. Excess heat capacities $\Delta C_p(=C_p(\text{glass}) - C_p(\text{crystal}))$ of OHMBBA. Base line: smoothed value of crystal. ○: crystal. ●: glassy liquid crystal.

crystal. This percentage gradually increases to 20% between 80 and 30 K and increases further as the temperature is lowered. Finally at the lowest temperature investigated here, the excess heat capacity amounted to as much as 50%. The peak centering around 25 K is probably attributed to the volumetric difference between the glassy and the crystalline state.(42) If a larger volume is occupied by a given amount of substance, the existing intermolecular forces would be weakened by the loose packing of molecules. This effect will bring about a change in the spectrum of the normal-mode-frequency distribution, that results in an increased heat capacity. This feature is conspicuous in the frequency spectra given in Fig. 4, where the normal modes with low-frequencies are abundantly distributed in the spectrum for the glassy state compared with that for the crystal.

It should be noted here that many investigators have neglected the difference between T_2 and T_0. In other words, they have regarded the heat capacities of the glassy state below T_g as the same with those of the crystalline state. But this is not the case in many glass-forming substances. Therefore, when the glass transition phenomena are discussed in terms of T_2 temperature, the related thermodynamic quantities for both the glassy and the crystalline states should be reduced to those under a certain common condition, say, under constant volume. The study of the excess heat capacity below T_g will provide other useful informations to aid the understanding of vitreous state.

In the meanwhile, it is interesting to compare the present glassy liquid crystal with the glassy liquids obtained from three of the 2,4-OHMBBA isomers. As was mentioned in Sec. 6, five isomers can be classified into two subgroups according to whether the hydrogen bonding is of an intra- or an inter-molecular nature. One group contains 2,3-, 2,4-, and 2,5-OHMBBA, and the other contains 3,4- and 4,3-OHMBBA. As given in Table 1, the only available data for comparison are the ratio of the glass transition temperature to the melting point T_g/T_m and the activation enthalpy of the glass transformation. It seems reasonable to compare these two quantities within the identical subgroup. As to the ratio T_g/T_m, there exists no remarkable difference among 2,3-, 2,4-, and 2,5-OHMBBA. On the other hand, the activation enthalpy of the glass transition, ΔH^*, for the liquid crystal of 2,4-OHMBBA is 10 $\sim$ 15 kJ mol^{-1} lower than that for 2,3- or 2,5-OHMBBA. If we take into consideration the similarity in molecular structure among these three, this difference may be attributed to the possible difference between the relaxational process of the glassy liquid crystal and that of the glassy liquid. Precise heat capacity measurements and also a knowledge of residual entropy at 0 K for 2,3- and 2,5-OHMBBA will provide other valuable information for the elucidation of the glassy liquid crystalline state.

Acknowledgements

The authors are grateful to Professor R. Kiriyama and Dr. K. Kitahama for permitting them to use a polarization microscope equipped with hot-stage.

REFERENCES

1. Kelker, H. and Scheurle, B., *Angew. Chem.* **81,** 903 (1969).
2. Teucher, I., Paleos, C. M. and Labes, M. M., *Mol. Cryst. and Liq. Cryst.* **11,** 187 (1970).
3. Rosenberg, H. M. and Champa, R. A., *Mol. Cryst. and Liq. Cryst.* **11,** 191 (1970).
4. Malthète, J., Leclercq, M., Gabard, J., Billard, J. and Jacques, J., *C.R. Acad. Sci.* (*Paris*), Ser. C, **273,** 265 (1971).
5. Champa, R. A., *Mol. Cryst. and Liq. Cryst.* **16,** 175 (1972).
6. Tsuji, K., Sorai, M. and Seki, S., not published. The heat capacities of cholesteryl hydrogen phthalate and cholesteryl myristate have been measured between 13 and 375 K.
7. Tsuji, K., Sorai, M. and Seki, S., *Bull. Chem. Soc. Japan* **44,** 1452 (1971).
8. Sorai, M. and Seki, S., *Bull. Chem. Soc. Japan* **44,** 2887 (1971).
9. Arnold, H., *Z. Phys. Chem.* **225,** 45 (1964); **226,** 146 (1965); with Roediger, P., **231,** 407 (1966); with El-Jazairi, E. B. and König, H., **234,** 401 (1967); with Roediger, P., **239,** 283 (1968); with Jacobs, J. and Sonntag, O., **240,** 177 (1969); with Demus, D., Koch, H. J., Nelles, A. and Sackmann, H., **240,** 185 (1969); *Z. Chem.* **4,** 211 (1964); *Mol. Cryst.* **2,** 63 (1966).
10. Barrall II, E. M., Porter, R. S. and Johnson, J. F., *J. Phys. Chem.* **68,** 2810 (1964); **70,** 385 (1966); **71,** 1224 (1967); *J. Chromatogr.* **21,** 392 (1966).
11. Ennulat, R. D., *Mol. Cryst.* **3,** 405 (1968); *Mol. Cryst. and Liq. Cryst.* **8,** 247 (1969).
12. Adachi, K., Suga, H. and Seki, S., *Bull. Chem. Soc. Japan* (a) **41,** 1073 (1968); (b) **43,** 1916 (1970); (c) **44,** 78 (1971); (d) **45,** 1960 (1972).
13. Schwartz, R. G. and Gerstein, B. C., *J. Chem. Phys.* **55,** 4034 (1971).
14. Matsuo, T., Oguni, M., Suga, H. and Seki, S., *Proc. Japan Acad.* **48,** 237 (1972).
15. Haida, O., Matsuo, T., Suga, H. and Seki, S., *Proc. Japan Acad.* **48,** 489 (1972).
16. This compound has not been yet put on the market by Tokyo Ohka Kogyo Co., Ltd. We are very grateful to Mr. B. Hori of this company for preparing this liquid crystal material for us.
17. Suga, H., Chihara, H. and Seki, S., *Nippon Kagaku Zasshi* **82,** 24 (1961).
18. Suga, H. and Seki, S., *Bull. Chem. Soc. Japan* **38,** 1000 (1965).
19 Westrum, E. F., Jr., Chou, C., Osborne, D. W. and Flotow, H. E., *Cryogenics* **7,** 43 (1967).
20. " The International Practical Temperature Scale of 1968 ", *Metrologia* **5,** 35 (1969).
21. McMillan, J. A., *J. Chem. Phys.* **42,** 3497 (1965).
22. Torgalkar, A., Porter, R. S., Barrall II, E. M. and Johnson, J. F., *J. Chem. Phys.* **48,** 3897 (1968).
23. Alben, R., *Mol. Cryst. and Liq. Cryst.* **10,** 21 (1970); **13,** 193 (1971).
24. Chandrasekhar, S. and Shashidhar, R., *Mol. Cryst. and Liq. Cryst.* **16,** 21 (1972).
25. Sorai, M. and Seki, S., *J. Phys. Soc. Japan* **32,** 382 (1972).

26. Brown, G. H., Doane, J. W. and Neff, V. D., *A Review of the Structure and Physical Properties of Liquid Crystals*, Butterworths, London (1971).
27. McMillan, W. L., *Phys. Rev.* **4A,** 1238 (1971).
28. Doane, J. W., Parker, R. S., Cvikl, B., Johnson, D. L. and Fishel, D. L., *Phys. Rev. Letters* **28,** 1694 (1972).
29. Litster, J. D. and Stinson III, T. W., *J. Appl. Phys.* **41,** 996 (1970).
30. Frenkel, J., *Kinetic Theory of Liquids*, Oxford University Press, London, 1947, Chap. VII.
31. Smith, J. W., *Electric Dipole Moments*, Butterworths Scientific Publications, London, 1955.
32. Chang, S. S., Horman, J. A. and Bestul, A. B., *J. Res. Nat. Bur. Stand.* **A71,** 293 (1967).
33. Simon, F. and Lange, F., *Z. Phys.* **38,** 227 (1926).
34. Chang, S. S. and Bestul, A. B., *J. Chem. Phys.* **56,** 503 (1972).
35. Sugisaki, M., Adachi, K., Suga, H. and Seki, S., *Bull. Chem. Soc. Japan* **41,** 593 (1968).
36. Counsell, J. F., Lees, E. B. and Martin, J. F., *J. Chem. Soc.* A 1819 (1968).
37. Sugisaki, M., Suga, H. and Seki, S., *Bull. Chem. Soc. Japan* **41,** 2586 (1968).
38. Huffman, H. M., Todd, S. S. and Oliver, G. D., *J. Amer. Chem. Soc.* **71,** 584 (1949).
39. Gibbs, J. H. and DiMarzio, E. A., *J. Chem. Phys.* **28,** 373 (1958).
40. Adam, G. and Gibbs, J. H., *J. Chem. Phys.* **43,** 139 (1965).
41. Angell, C. A., *J. Amer. Ceram. Soc.* **51,** 117 (1968); **51,** 125 (1968).
42. Guttman, C. M., *J. Chem. Phys.* **56,** 627 (1972).